Blind Carrier Frequency Offset Estimation Based on Eighth-Order Statistics for Coherent Optical QAM Systems

Ming Li and Lian-Kuan Chen, *Senior Member, IEEE*

***Abstract*—We propose a carrier frequency offset estimation (FOE) algorithm based on eighth-order statistics for optical quadrature amplitude modulation (QAM) signals. The FOE algorithm does not involve fast Fourier transformation and can be implemented by hardware with little memory and computation resources. Simulation results show that in a 10.709-GBaud/s optical 16-QAM system, carrier frequency offset ranging between $\pm$1.25 GHz can be estimated with a uniform standard deviation of 2 MHz when the optical signal-to-noise ratio is 17 dB and 4^{10} symbols are utilized.**

***Index Terms*—Coherent detection, frequency estimation, optical fiber communication, quadrature amplitude modulation (QAM).**

I. Introduction

THE ever growing demand for high-speed data transmission is one of the major factors that fuel the development of high-capacity optical fiber communication systems and networks. To make most use of transmission links that have already been deployed, system capacity can be upgraded by utilizing multilevel modulation formats. Succeeding M-ary phase shift keying (M-PSK), quadrature amplitude modulation (QAM) is a promising modulation format to economically increase the number of bits carried by each symbol [1], [2].

To avoid using complex optical phase locked loops, in most cases optical QAM signal is coherently detected with an optical local oscillator (OLO) running independently from the transmitter laser. Therefore, the phase noise of the optical carrier needs to be estimated and compensated before symbol decision. Unfortunately, the tolerance of carrier frequency offset for most carrier phase estimation (CPE) algorithms is limited, for example decision-directed CPE for 14-GBaud/s 16-QAM signal can only tolerate a frequency offset of 100 MHz [2]. Hence it is preferable to estimate and compensate carrier frequency offset prior to CPE so that the requirement of the center frequency alignment between the transmitter laser and the OLO can be relaxed [3]–[8].

Without training symbols, optical carrier frequency offset estimation (FOE) can be performed by comparing phases of coherently detected adjacent symbols after data modulation removal, which can be performed by Mth power operation [3], modulus operation [4], or predecision [5] for optical M-PSK signals. However, for optical QAM signals data modulation removal is difficult because the phases representing data modulation are no longer equally distributed between 0 and 2π. Nevertheless, carrier FOE for optical QAM signals can be performed by searching the maximum of the periodogram of the samples after 4th power operation [6], [7] , or by searching the maximum of the periodogram of the samples' argument after selective rotation [8], both involving fast Fourier transformation (FFT) which consumes considerable memory and computation resources when implemented with hardware such as field programmable gate array (FPGA).

In this letter, we propose a carrier FOE algorithm based on eighth-order statistics for optical QAM signals. Compared with the algorithms based on periodogram, the algorithm consumes substantially less memory resources because the statistics can be computed based on current and the last symbols and no other symbols need to be buffered. Since the algorithm does not require large-scale parallel computation, it also consumes less computation resources, albeit at the expense of larger number of symbols used.

II. FOE Algorithm and Simulation Setup

The FOE algorithm is based on the blind CPE algorithm proposed by Cartwright [9]. For optical QAM signal the kth coherently detected and dispersion compensated symbol before FOE can be represented by

$$Y^{(k)} = Y_r^{(k)} + jY_i^{(k)} = e^{j\theta_k} X^{(k)} + n^{(k)}, \tag{1}$$

where $X^{(k)} = X_r^{(k)} + jX_i^{(k)}$ is the transmitted symbol, $n^{(k)} = n_r^{(k)} + jn_i^{(k)}$ is the Gaussian additive noise, and θ_k is the phase difference between the optical carrier and the OLO, respectively. If we write

$$\begin{aligned} Z_r^{(k)} &= [Y_r^{(k)}]^4 + [Y_i^{(k)}]^4 - 6[Y_r^{(k)}]^2[Y_i^{(k)}]^2 \\ Z_i^{(k)} &= 4[Y_r^{(k)}]^3 Y_i^{(k)} - 4Y_r^{(k)}[Y_i^{(k)}]^3, \end{aligned} \tag{2}$$

and under the assumptions that

$$\begin{aligned} E\{X_r^{(k)} X_i^{(k)}\} &= 0 \\ E\{X_r^{(k)}\} = E\{X_i^{(k)}\} &= 0 \\ E\{[X_r^{(k)}]^2\} &= E\{[X_i^{(k)}]^2\} \\ E\{[X_r^{(k)}]^3 X_i^{(k)}\} &= E\{X_r^{(k)}[X_i^{(k)}]^3\}, \end{aligned} \tag{3}$$

Manuscript received June 11, 2011; revised July 24, 2011; accepted August 05, 2011. Date of publication August 15, 2011; date of current version October 12, 2011. This work was supported in part by research grants from the Hong Kong Research Grants Council (Project 410910).

The authors are with the Department of Information Engineering, The Chinese University of Hong Kong, Shatin, N. T., Hong Kong SAR, China (e-mail: mingli@ie.cuhk.edu.hk; lkchen@ie.cuhk.edu.hk).

Digital Object Identifier 10.1109/LPT.2011.2164788

the expectation of $Z^{(k)} = Z_r^{(k)} + jZ_i^{(k)}$ would be [9]

$$E\{Z^{(k)}\} = \gamma_x e^{j4\theta_k}, \tag{4}$$

in which

$$\gamma_x = E\{[X_r^{(k)}]^4\} + E\{[X_i^{(k)}]^4\} - 6E\{[X_r^{(k)}]^2[X_i^{(k)}]^2\}. \tag{5}$$

Since the dispersion has been fully compensated, we can further assume $Z^{(k)}$ and $Z^{(k+1)}$ are statistically independent. The expectation of $[Z^{(k)}]^* Z^{(k+1)}$ would be

$$E\{[Z^{(k)}]^* Z^{(k+1)}\} = E\{[Z^{(k)}]^*\}E\{Z^{(k+1)}\} = \gamma_x^2 e^{j4(\theta_{k+1}-\theta_k)}. \tag{6}$$

Thus we can derive the carrier frequency offset estimator as

$$\widehat{\Delta f} = \frac{\arg\left\{\sum_k [Z^{(k)}]^* Z^{(k+1)}\right\}}{8\pi T}, \tag{7}$$

where T is the symbol duration.

The above assumptions are valid for 16-QAM signals even when the differential encoding scheme in [1] is used. Noting that the probability associated with each point in the constellation remains to be the same when the differential encoding scheme is used, assumptions in (3) can be easily verified. As for statistical independence of $Z^{(k)}$ and $Z^{(k+1)}$, we only need to show that $X^{(k)}$ and $X^{(k+1)}$ are statistically independent. This can be verified by calculating marginal distributions as well as joint distribution of $X^{(k)}$ and $X^{(k+1)}$, bearing in mind that the transition between any pair of $X^{(k)}$ and $X^{(k+1)}$ is equally probable.

We evaluate the performance of the FOE algorithm in a 10.709-GBaud/s optical 16-QAM system by simulation. In the transmitter two random quaternary sequences generated by MATLAB are combined and differentially encoded before being modulated on a transmitter laser with 100-kHz linewidth to generate optical 16-QAM signal. Dispersion impairments are not considered because they are supposed to be compensated before FOE. Amplified spontaneous emission (ASE) noise is added to adjust the optical signal-to-noise ratio (OSNR). After passing through a 50-GHz second-order super-Gaussian optical bandpass filter (OBPF), the optical signal is coherently detected with an OLO of 100-kHz linewidth. We assume the receiver has fifth-order Bessel low-pass characteristics and its 3-dB bandwidth is 9 GHz. Finally carrier FOE is performed and the mean μ_e and standard deviation (STD) σ_e of its error are calculated based on 500 runs of simulation.

III. Simulation Results

We first simulate the case when the carrier frequency offset is fixed to 500 MHz and the optical signal is not distorted by dispersion. Figs. 1(a) and 1(b) show the estimated mean μ_e and STD σ_e of the FOE error as functions of the number of symbols utilized when the optical signal is not contaminated by ASE noise. Calculated with Monte Carlo simulation, the estimated μ_e and σ_e are random variables which converge to the corresponding true values with probability one as the number of runs of simulation approaches infinity. The difference between the estimated μ_e and σ_e curves for laser linewidths $\Delta\nu$ of up to 1 MHz is negligible, while the curves for laser linewidth of 10 MHz are for reference only. When the laser linewidth is less than or equal to 1 MHz, μ_e is less than 500 kHz, which can be neglected with regard to the frequency offset tolerance of the CPE algorithms. As the number of symbols increases by a factor of four, σ_e reduces by half. This coincides with the fact that the variance of the average of a set of uncorrelated and identical distributed random variables is inversely proportional to the number of the random variables. With 4^{10} symbols σ_e is roughly 1.3 MHz for a laser linewidth of less than or equal to 1 MHz. Figs. 1(c) and 1(d) show the estimated μ_e and σ_e as functions of the signal OSNR. When 4^{10} symbols are utilized $(N = 4^{10})$ μ_e ranges between ± 250 kHz as the OSNR varies from 14 dB to 22 dB, which indicates that μ_e does not increase significantly when the ASE noise is included. For the case of 4^8 symbols, due to the larger variance of the FOE error, 500 runs of Monte Carlo simulation is inadequate to provide an accurate estimation of its distribution. σ_e rises with decreasing OSNR and a roughly 50% increase of σ_e can be observed when the OSNR falls from infinity, shown in Fig. 1(b), to 17 dB, which corresponds to 10^{-3} bit error rate [1]. Increasing the number of symbols by a factor of four still reduces σ_e by half.

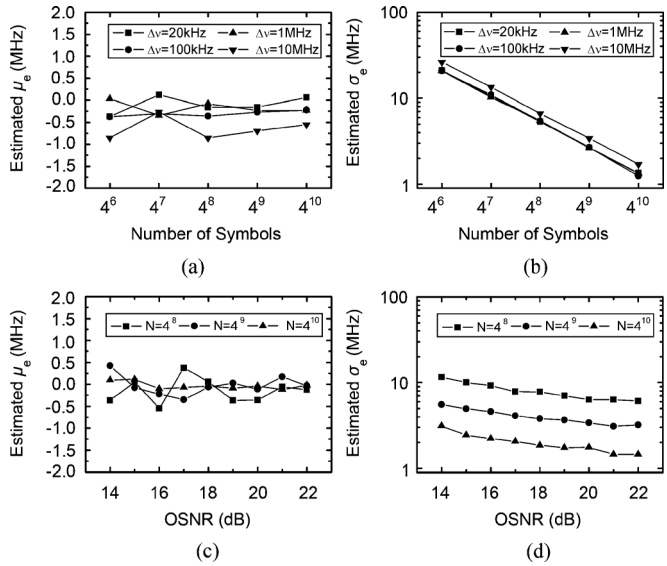

Fig. 1. Estimated (a) mean and (b) STD of the FOE error as functions of the number of symbols utilized when the optical signal is free of ASE noise; estimated (c) mean and (d) STD of the error as functions of the OSNR.

We then simulate the case when the optical signal is distorted by chromatic dispersion (CD) or differential group delay (DGD) and show the results in Fig. 2. In the simulation the carrier frequency offset is still 500 MHz, the OSNR is 17 dB, and 4^{10} symbols are utilized for the carrier FOE. Due to the distortion of the constellation points by dispersion, μ_e drifts at the presence of CD and DGD. When the CD is between ± 1000 ps/nm μ_e varies between ± 3 MHz, and μ_e is within ± 1.5 MHz for a DGD up to 50 ps. σ_e is less sensitive to the dispersion, and it is less than 4 MHz and 2.5 MHz in the aforementioned CD and DGD range, respectively.

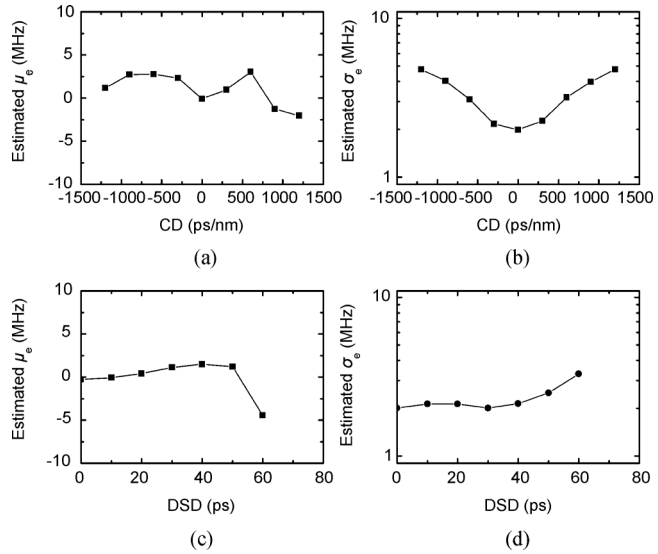

Fig. 2. Estimated (a) mean and (b) STD of the FOE error as functions of the CD; estimated (c) mean and (d) STD of the error as functions of the DGD.

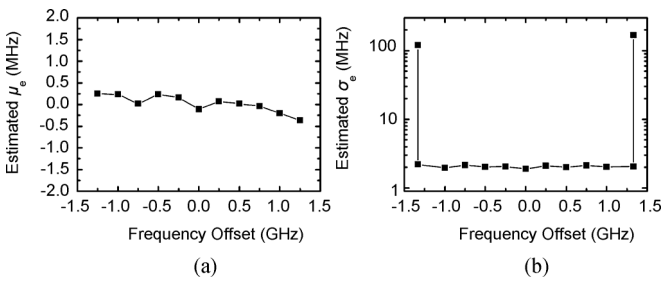

Fig. 3. Estimated (a) mean and (b) STD of the FOE error as functions of the carrier frequency offset.

Fig. 3 shows μ_e and σ_e as functions of the carrier frequency offset when the OSNR of the optical signal is 17 dB and 4^{10} symbols are utilized. As the carrier frequency offset varies between ± 1.25 GHz σ_e remains to be around 2 MHz, but it rises abruptly when the carrier frequency offset approaches $-1/8T$ and $1/8T (1/8T \approx 1.34$ GHz). This is because the range of the estimator in (7) is $(-1/8T, 1/8T]$ and the estimated carrier frequency offset will be wrapped if it is out of the range. When the carrier frequency offset varies between ± 1.25 GHz μ_e changes slightly. Confirmed by simulation results that are not shown here due to limited space, this variation is because the positive frequency and negative frequency parts of the signal are asymmetrically filtered when the carrier frequency offset is not zero. Nevertheless, μ_e is within ± 250 kHz and the effect on the following CPE can be neglected. The estimated μ_e when the carrier frequency offset approaches $-1/8T$ and $1/8T$ is not shown in Fig. 3(a) because its magnitude is too large.

Finally we estimate and compare the hardware resource requirement of the FOE algorithm based on periodogram and that of the proposed FOE algorithm. Assuming the radix-2 burst I/O architecture [10], the FOE algorithm based on N-point periodogram would need memory to store $2N$ real numbers for the samples and roughly $2N$ real numbers for the phase factors. Since the FFT core includes $N/2$ butterflies, each of which has four real multipliers and six real adders, the FOE algorithm based on N-point periodogram would require $2N$ real multipliers and $3N$ real adders. In addition, the FOE algorithm based on N-point periodogram needs switches to dynamically configure the butterflies for different stages in the transformation. As for the proposed FOE algorithm, we assume a parallel-pipeline architecture which can finish processing the samples right after they have been received. When the number of the parallel branches is P, the proposed algorithm would need memory to store $9P$ real numbers for intermediate results and two real numbers for the estimator. Since in each parallel branch 13 real multipliers and 7 real adders are needed, the proposed algorithm requires a total number of $13P$ real multipliers and $7P$ real adders. As can be seen from above, when the number of samples to be processed increases, the FOE algorithm based on periodogram needs more hardware resources; while for the proposed algorithm the required hardware resources is fixed, but a longer waiting time is needed.

IV. Conclusion

We have proposed and investigated a simple FOE algorithm based on eighth-order statistics for optical QAM signal. When implemented with hardware such as FPGA, the algorithm consumes substantially less memory and computation resources than the algorithms based on periodogram. Simulation results show that utilizing 4^{10} symbols of a 10.709-GBaud/s optical QAM signal with 17-dB OSNR, the FOE algorithm can achieve a uniform 2-MHz STD of the FOE error when the carrier frequency offset varies between ± 1.25 GHz. The carrier FOE algorithm is a competitive candidate for the implementation of carrier FOE in QAM optical coherent receivers, especially when the hardware resources is limited.

References

[1] T. Pfau, S. Hoffmann, and R. Noé, "Hardware-efficient coherent digital receiver concept with feedforward carrier recovery for M-QAM constellations," *J. Lightw. Technol.*, vol. 27, no. 8, pp. 989–999, Apr. 15, 2009.

[2] P. J. Winzer, A. H. Gnauck, C. R. Doerr, M. Magarini, and L. L. Buhl, "Spectrally efficient long-haul optical networking using 112-Gb/s polarization-multiplexed 16-QAM," *J. Lightw. Technol.*, vol. 28, no. 4, pp. 547–556, Feb. 15, 2010.

[3] A. Leven, N. Kaneda, U.-V. Koc, and Y.-K. Chen, "Frequency estimation in intradyne reception," *IEEE Photon. Technol. Lett.*, vol. 19, no. 6, pp. 366–368, Mar. 15, 2007.

[4] S. Hoffmann, S. Bhandare, T. Pfau, O. Adamczyk, C. Wördehoff, R. Peveling, M. Porrmann, and R. Noé, "Frequency and phase estimation for coherent QPSK transmission with unlocked DFB lasers," *IEEE Photon. Technol. Lett.*, vol. 20, no. 18, pp. 1569–1571, Sep. 15, 2008.

[5] L. Li, Z. Tao, S. Oda, T. Hoshida, and J. C. Rasmussen, "Wide-range, accurate and simple digital frequency offset compensator for optical coherent receivers," in *Proc. Optical Fiber Commun. Conf. (OFC)*, San Diego, CA, 2008, Paper OWT4.

[6] M. Selmi, Y. Jaouën, and P. Ciblat, "Accurate digital frequency offset estimator for coherent PolMux QAM transmission systems," in *Proc. Eur. Conf. Optical Commun. (ECOC)*, Vienna, Austria, 2009, Paper P3.08.

[7] T. Nakagawa, M. Matsui, T. Kobayashi, K. Ishihara, R. Kudo, M. Mizoguchi, and Y. Miyamoto, "Non-data-aided wide-range frequency offset estimator for QAM optical coherent receivers," in *Proc. Optical Fiber Commun. Conf. (OFC)*, Los Angeles, CA, 2011, Paper OMJ1.

[8] Y. Cao, S. Yu, Y. Chen, Y. Gao, W. Gu, and Y. Ji, "Modified frequency and phase estimation for M-QAM optical coherent detection," in *Proc. Eur. Conf. Optical Commun. (ECOC)*, Torino, Italy, 2010, Paper We.7.A.1.

[9] K. V. Cartwright, "Blind phase recovery in general QAM communication systems using alternative higher order statistics," *IEEE Signal Process. Lett.*, vol. 6, no. 12, pp. 327–329, Dec. 1999.

[10] Xilinx DS808 LogiCORE IP FFT v8.0 Datasheet. Xilinx Inc., San Jose, CA, 2011.